Exploring interactions between pectins and procyanidins: Structure-function relationships

Xuwei Liu, Catherine M.G.C. Renard, Agnès Rolland-Sabaté, Carine Le Bourvellec

Exploring interactions between pectins and procyanidins: Structure-function relationships

Xuwei Liu[a], Catherine M.G.C. Renard[a,b], Agnès Rolland-Sabaté[a], Carine Le Bourvellec[a]*

[a]INRAE, Avignon University, UMR408 SQPOV, F-84000 Avignon, France

[b]INRAE, TRANSFORM, F-44000 Nantes, France

Corresponding authors*

Carine Le Bourvellec (carine.le-bourvellec@inrae.fr)

INRAE, UMR408 SQPOV « Sécurité et Qualité des Produits d'Origine Végétale »

228 route de l'Aérodrome

CS 40509

F-84914 Avignon cedex 9

Tél: +33 (0)4 32 72 25 35

Fax: +33 (0)4 32 72 24 92

Others authors

Xuwei Liu: xuwei.liu@inrae.fr

Catherine M.G.C Renard: catherine.renard@inrae.fr

Agnès Rolland-Sabaté: agnes.rolland-sabate@inrae.fr

Abstract

During fruit and vegetable processing, procyanidins interact with cell walls and form complexes, which further impact their potential health effects. Among cell wall polysaccharides, pectins have the highest affinity for procyanidins. Binding of two procyanidin fractions with twelve pectins of different linearity and size was investigated by ITC, UV-Visible spectrophotometry and HPSEC-MALLS. Pectins interacted preferentially with highly polymerized procyanidins except beet pectins probably because of steric hindrance due to abundant feruloylated arabinans. Linear pectins had higher affinity for procyanidins: this was verified both for comparison between botanical origins (kiwifruit > apple > beet pectins) and between extraction conditions. Debranched pectins, extracted at pH 2.0, had higher affinity and aggregation capacities with procyanidins than those extracted at other pHs. However, the factors affecting pectins of different origins seemed to be different. High molar mass, intrinsic viscosity and hydrodynamic radius contributed more to increased adsorption of procyanidins by apple and beet pectins. Highly linear kiwifruit pectins, with high homogalacturonan content and lower branching ratio bound preferentially to procyanidins. The enthalpy/entropy proportion of the interaction between kiwifruit pectins and procyanidins was higher than that of apple and beet pectins, which suggested more hydrogen bonding. Predominance of homogalacturonan regions and high degree of methylation thus appeared key structural features of pectins for high affinity for procyanidins, while high degree of branching was detrimental. These findings provide the structural foundation for selectivity of interactions in molecular-level.

Keywords: polyphenol, condensed tannins, polysaccharide, homogalacturonan rhamnogalacturonan, methylation, association

Abbreviations:

HPSEC-MALLS, High Performance Size-Exclusion Chromatography combined with Multi-Angle Laser Light Scattering; AIS, Alcohol Insoluble Solids; Isothermal Titration Calorimetry, ITC; $\overline{[\eta]}_z$, z-average intrinsic viscosity; $\overline{R}_{Hz}$, z-average

hydrodynamic radius; $\bar{R}_{Hw}$, weight-average hydrodynamic radius; $\bar{M}_{w}$, weight-average molar mass; $\bar{d}_{Happ}$, weight-average apparent molecular density; homogalacturonan, HG; rhamnogalacturonan of type I, RG-I.

1. Introduction

In plant-based food systems (such as fruits, vegetables, and grains), secondary metabolites (e.g., polyphenols) and macromolecules (e.g., proteins and polysaccharides) coexist in strictly compartmented parts of the plant cells and commonly come in contact with each other during processing, mastication and digestion (Le Bourvellec et al., 2019; Le Bourvellec & Renard, 2012). Structure-function relationships of the main non-digestible biologically active components in plant-based functional foods, polysaccharides and polyphenols, may be regulated by their interactions (Dobson et al., 2019; Kardum & Glibetic, 2018). Dietary polysaccharide-polyphenol interactions might affect the physical properties of polysaccharides, e.g., texture and stability, in food systems (Jin et al., 2020; Li, Liu, Tu, Li, & Yan, 2019; Liu, Le Bourvellec, & Renard, 2020; Tudorache & Bordenave, 2019; Tudorache, McDonald, & Bordenave, 2020) as well as their biological activity (Le Bourvellec et al., 2019). In addition, the bioaccessibility, bioavailability and bioefficacy of polyphenols depends on their interaction with other food ingredients, e.g., dietary fiber in particular (Ribas-Agustí, Martín-Belloso, Soliva-Fortuny, & Elez-Martínez, 2018). Such dietary fibers, e.g., apple matrix, apple cell wall (Le Bourvellec et al., 2019; Monfoulet et al., 2020) and pure cellulose (Phan et al., 2020), can be used as a carrier for polyphenols to transport these antioxidants to the human gut microbiota and further produce beneficial physiological effects after their fermentation in small phenolic compounds (Loo, Howell, Chan, Zhang, & Ng, 2020; Saura-Calixto, 2011).

Plant polyphenols have at least one aromatic ring and one or more hydroxyl groups (phenol group), ranging from simple phenolic acids to complex flavonoids. Procyanidins, also known as condensed tannins, are a type of proanthocyanidins and in particular they have a high affinity for polysaccharides. They are polymers and oligomers of catechin/epicatechin (flavan-3-ol units) and most commonly connected by B-type bonds, namely C4-C8 or C4-C6 interflavanic linkages with a number average degree of polymerization ($\overline{DP}n$) varying between 2 and more than 100 (Guyot, Marnet, & Drilleau, 2001). The interactions between macromolecules and procyanidins are dependent on their structural characteristics, i.e. molar mass, interflavanic bonds, the presence of galloyl groups and conformation (Le Bourvellec & Renard, 2019; Liu et al., 2020). In general, their affinity for polysaccharides increases with their $\overline{DP}n$ and molar mass (Le Bourvellec, Guyot, & Renard, 2004; Le Bourvellec & Renard, 2005, 2012; Mamet, Ge, Zhang, & Li, 2018; Renard, Baron, Guyot, & Drilleau, 2001). For example, procyanidins have been demonstrated to bind strongly to pectins, a major constituent of most fruit and vegetable plant cell walls (Le Bourvellec & Renard, 2005; Liu et al., 2020; Renard et al., 2001). Increasing the level of galloylation of procyanidins also enhances their affinity with pectins due to the increased number of hydroxyl groups and aromatic rings (Le Bourvellec et al., 2004; McManus et al., 1985; Tang, Covington, & Hancock, 2003). (+)-Catechin and polymers composed mainly of (+)-catechin units bind more to polysaccharides than (-)-epicatechin and polymer composed mainly of (-)-epicatechin due to the stereochemistry of flavan-3-ols pyran rings (Le Bourvellec et al., 2004).

Pectins are complex polysaccharides widely found in primary plant cell walls, and are acid hetero-polysaccharides. The pectic polysaccharides contain three main structural units as follows. Homogalacturonan (HG) is a long and smooth chains of linear α-1,4-linked D-galacturonic acid, in which most of the C-6 carboxyl groups are methyl-esterified and some of the secondary alcohols at the O-2 and/or the O-3 positions may be acetyl-esterified (Caffall & Mohnen, 2009; Mohnen, 2008; Ridley, O'Neill, & Mohnen, 2001). Rhamnogalacturonan-I (RG-I) is composed of a backbone of repeating units of galacturonic acid and rhamnose linked by α-1,2 and α-1,4 glycosidic bonds: [→4)-α-D-GalpA-(1→2)-α-L-Rhap-(1→] and may be substituted at the O-2 and/or the O-3 positions of α- L -rhamnose residues (Mohnen, 2008; Voragen, Coenen, Verhoef, & Schols, 2009). Rhamnogalacturonan II (RG-II), making up ~10% of pectins, is the most structurally complex and branched polysaccharide in this family of pectic polysaccharides (Caffall & Mohnen, 2009; Ridley et al., 2001). The highly complex polymer structure of RG-II is composed of an HG backbone of seven to nine (and most probably more) 1,4-linked α-D-Gal-A residues including four side chains clearly consisting of 12 different kinds of monosaccharides through more than 20 different linkages (Pérez, Rodríguez-Carvajal, & Doco, 2003). Pectins with high degree of methylation (DM) display the strongest affinity for procyanidins due to hydrophobic interactions, while highly branched pectins have more limited interactions with procyanidins, probably due to steric hindrance (Watrelot, Le Bourvellec, Imberty, & Renard, 2013, 2014). Pectins, especially HG, are susceptible to various enzymatic and non-enzymatic conversion reactions during processing of

plant-based products, modifying their structure and, hence, their physicochemical properties (Dongowski, 2001; Fraeye et al., 2007; Renard & Thibault, 1996), which in turn may affect their interaction with procyanidins (Le Bourvellec, Watrelot, Ginies, Imberty, & Renard, 2012).

Interactions of procyanidins has been studied with pectins of different commercial origins (apple or citrus) or with pectin structural units. Higher affinities were recorded for citrus pectins or for highly methylated homogalacturonans (Watrelot et al., 2013), while type I rhamnogalacturonans with different side-chains (Watrelot et al., 2014) or arabinans (Fernandes et al., 2020) had lower affinities. Also, different pectin components will interact in a complex manner determining the fine structure of the biopolymer (e.g., hydrogen, hydrophobic, or ionic bonding) and its spatial conformation (Janaswamy & Chandrasekaran, 2005; Pérez, Mazeau, & Hervé du Penhoat, 2000) that will further affect their interaction with procyanidins (Watrelot et al., 2014). However, there is little systematic information on the effect of native pectin's structural features (both composition and spatial conformation) on their interaction with procyanidins, particularly involving combinations of light scattering and spectroscopy techniques, and together with thermodynamics. Therefore, the determination of the impact of conformational properties and composition of pectins is crucial. To do this, pectins differing for their main structural features, i.e. molar mass, size, proportion of branching, length and content of HG, HG / RG ratio and degrees of methylation and acetylation, were used to gain in-depth understanding of the structure/function relationships that govern their interactions with procyanidins.

For this, a series of twelve pectins with different HG / RG ratios, side-chains and esterifications was prepared by extraction from apple, beet and kiwifruit (two maturities for kiwifruit) cell walls at pH 2.0, 3.5, and 6.0. These twelve different pectins were incubated with procyanidins solutions of intermediate and high $\overline{DP}n$, DP9 and DP79, respectively. Interactions were characterized by aggregates formation using UV−visible spectroscopy and by isothermal titration calorimetry. The pectin macromolecular characteristics before and after interactions were determined by size-exclusion chromatography coupled with multi-angle laser light scattering and viscometric detections to better understand the selectivity of their interactions with procyanidins. A deep understanding of the molecular mechanisms that drive the interaction between pectins and procyanidins can enable us to better bridge the gap between food processing and the bioavailability of commensal microbiota fermentation products of pectin and procyanidins. Further, this promotes the design of more rational processing conditions and healthier and more nutritious foods.

2. Materials and methods

2.1. Standards and Chemicals

Ethanol and acetone were provided from Fisher Scientific (Strasbourg, France). Acetonitrile, methanol of HPLC grade were obtained from VWR International (Radnor, USA). Hexane was from Merck (Darmstadt, Germany). Sugar standards (arabinose, fucose, galactose, xylose, mannose and rhamnose) were from Fluka (Buchs, Switzerland). Methanol-d_3 was from Acros Organics (Geel, Belgium). Formic

142 acid, chlorogenic acid, benzyl mercaptan, sodium carbonate, sodium hydroxide,
143 $NaBH_4$, N-methylimidazole, acetic anhydride, toluene-α-thiol, (+)-catechin and
144 (-)-epicatechin were from Sigma-Aldrich (Saint Quentin Fallavier, France).
145 4-Coumaric acid was obtained from Extrasynthese (Lyon, France). Phloridzin was
146 obtained from Fluka (Buchs, Switzerland).

147 **2.2. Extraction, purification and characterization of procyanidins**

148 **2.2.1. Plant material**

149 Apple fruits (*Malus* × *domestica* Borkh.) from the 'Marie Menard' and 'Avrolles'
150 cider cultivars were harvested at maturity (after starch regression) in the experimental
151 orchard of the Institut Français des Productions Cidricoles (Sées, Orne, France). Fruits
152 were mechanically cored and a formic acid solution (10 mL/L) was sprayed on the
153 fresh material to avoid phenolic oxidation. Cortex tissues were then frozen,
154 freeze-dried, and stored at -20 °C until used.

155 **2.2.2. Procyanidin extraction and purification**

156 Apple polyphenols were extracted from the freeze-dried apple powder (150 g)
157 sequentially by hexane, methanol and aqueous acetone according to a procedure
158 described by (Guyot et al., 2001). Hexane and methanol extracts were discarded as
159 they did not contain the required procyanidin fractions and to eliminate lipids, sugars,
160 organic acids and phenolic compounds of low molar mass. Aqueous acetone extracts
161 containing procyanidins were pooled and concentrated on a rotary evaporator prior to
162 freeze-drying. The freeze-dried aqueous acetone extracts were dissolved (100 g/L) in

163 water acidified with formic acid (99.9:0.1, v/v), centrifuged (16 800 x *g*, 15 min) and
164 then filtered. They were injected on a 20×5 cm column of LiChrospher 100 RP-18 (12
165 µm, Merck, Darmstadt, Germany) and purified as described by Brahem, Renard,
166 Bureau, Watrelot, & Le Bourvellec (2019). Procyanidin fractions were concentrated
167 on a rotary evaporator then freeze-dried and stored under vacuum at -80 °C until used.
168 The purified procyanidin fractions are designated as DP9 (from 'Marie Ménard') and
169 DP79 (from 'Avrolles').

170 **2.2.3. Procyanidin characterizations**

171 Procyanidins were analyzed by high-performance liquid chromatography (HPLC)
172 with diode array detection (DAD) with or without thioacidolysis as described by
173 Guyot et al. (2001). Analysis were performed using the ultra-fast liquid
174 chromatography and controlled by LC Solution software (Shimadzu Prominence
175 system, Kyoto, Japan). The system was operated by two LC-20AD pumps
176 Prominence LC UFLC, a DGU-20A5 Prominence degasser, a SIL-20ACHT
177 Prominence autosampler, a CTO-20AC Prominence column oven, an SPD-M20A
178 Prominence diode array detector and a CBM-20A Prominence communication bus
179 module. Separations were achieved as described in Le Bourvellec et al. (2011). The
180 average degree of polymerization of procyanidins ($\overline{DP}n$) was calculated as the molar
181 ratio of all flavan-3-ol units (thioether adduct plus terminal units minus (+)-catechin
182 and (-)-epicatechin naturally present in the samples and determined by analysis of the
183 samples without thiolysis) to (+)-catechin and (-)-epicatechin corresponding to the
184 terminal units minus (+)-catechin and (-)-epicatechin naturally present in the samples

and determined by analysis of the samples without thiolysis.

2.3. Preparation of pectin fractions

Pectins from apple (A-), beet (B-) and kiwifruits (K-) (ripe R- and overripe O-) were prepared as described by (Liu, Renard, Rolland-Sabaté, Bureau, & Le Bourvellec, 2021). Cell walls were isolated from the parenchyma of the different edible plant materials as alcohol insoluble solids. Subsequently, pectins were extracted from each cell wall material by boiling for 20 min in a citrate-phosphate solution (0.1 M) at three pH values: 2.0, 3.5 and 6.0. Thus, twelve pectin fractions were obtained. That is, apple, beet, kiwifruit (ripe) and kiwifruit (overripe) pectins extracted at pH 2.0/3.5/6.0 were designated AP2/3/6, BP2/3/6, KPR2/3/6 and KPO2/3/6, respectively. The purpose of this step is to obtain pectins of different compositions and structures.

2.4. Initial and free pectin macromolecular characteristics

The pectins (2.5 g/L) were analyzed by High Performance Size-Exclusion Chromatography coupled with Multi-Angle Laser Light Scattering (HPSEC-MALLS) after being filtered as described by Liu et al. (2021). Samples (100 µL) were injected and the mobile phase was 0.1 M citrate/phosphate buffer with pH 3.8, and eluted at 0.6 mL/min. The system comprised three HPSEC columns (PolySep-GFC-P3000, P5000 and P6000, 300 ×7.8 mm) and a guard column from Phenomenex (Le Pecq, France) maintained at 40 °C, a MALLS detector (DAWN HELEOS 8+ fitted with a K5 flow cell and a GaAs laser (λ = 660 nm), a Viscostar III viscometer, both from

206 Wyatt Technology Corporation (Santa Barbara, CA, USA), a diode array detector
207 (SPD-M20A) and a fluorescence detector (RF-20A) set at 360 nm (280 nm excitation)
208 and a refractive index detector (RID-10A) from Shimadzu (Shimadzu Prominence
209 system, Kyoto, Japan).

210 M_i and R_{Gi}, the molar mass and the radius of gyration at each slice of the
211 chromatogram, was determined using the concentration (calculated from the
212 refractometric signal) and the light scattering signal from 5 angles (from 20.4° to 90°)
213 and data extrapolation to zero angle using the Zimm formalism with a one order
214 polynomial fit (Rolland-Sabaté, Colonna, Potocki-Véronèse, Monsan, & Planchot,
215 2004) using ASTRA® software from Wyatt Technology Corporation (version 7.1.4 for
216 PC). R_{hi}, the viscometric hydrodynamic radius at each slice of the chromatogram for
217 the equivalent sphere, was calculated by combining viscosity and molar mass
218 measurements using the following equation derived from the Einstein and Simha
219 relation (Einstein, 1906, 1911; Simha, 1940):

220 $$[\eta]_i M_i = \gamma N_A V_{hi} = \frac{10\pi}{3} N_A R_{hi}^3 \qquad (1)$$

221 where $[\eta]_i$ and V_{hi} are the intrinsic viscosity and the hydrodynamic volume at
222 each slice of the chromatogram, $\gamma = 2.5$ for spheres and N_A the Avogadro number.

223 The z-average intrinsic viscosity ($\overline{[\eta]}_z$), z-average and weight average viscometric
224 hydrodynamic radii ($\overline{R}_{Hz}$ and $\overline{R}_{Hw}$) and weight-average molar mass ($\overline{M}_w$) were
225 established using the averaging described in Rolland-Sabaté *et al.* (Rolland-Sabaté et
226 al., 2004; Rolland-Sabaté, Mendez-Montealvo, Colonna, & Planchot, 2008) on the
227 whole peaks. A value of 0.146 mL/g was used as the refractive index increment (dn/dc)

for glycans and the normalization of photodiodes was achieved using a low molar mass pullulan standard (P20) from Showa Denko K.K. (Tokyo, Japan). The average apparent molecular density ($\bar{d}_{Happ}$) was calculated using the following equation:

$$\bar{d}_{Happ}=\overline{M_w}/(4\pi/3) * \overline{R}^3_{Hw} \quad (2)$$

The log-log plot of hydrodynamic radius versus the molar mass and the Mark-Houwink-Sakurada plot were established for each sample by using the data taken at each slice of the chromatogram. The power law exponent (α) can be calculated according to the following equations:

$$[\eta]_i = K_a M_i^{\alpha} \quad (3)$$

where K_a is a constant and α is the hydrodynamic coefficient which depends on the polymer shape in the solvent.

2.5. Phase Diagram

The formation of aggregates was analyzed by spectrophotometry during the pectin-procyanidin interactions as described by Watrelot et al. (2013). All measurements were done in duplicates. The turbidity measurements were carried out with a SAFAS flx-Xenius XM spectrofluorimeter (SAFAS, Monaco) at 650 nm on a 96-well microplate at 25 °C. A serial procyanidin solutions (0, 0.03, 0.06, 0.12, 0.24, 0.47, 0.94, 1.875, 3.75, 7.5, 15 and 30 mmol/L (-)-epicatechin equivalent for 'Avrolles'; 0, 0.06, 0.12, 0.24, 0.46, 0.94, 1.875, 3.75, 7.5, 15, 30 and 60 mmol/L (-)-epicatechin equivalent for 'Marie Ménard') and pectins (0, 0.015, 0.03, 0.06, 0.24, 0.94, 3.75 and 15 mmol/L galacturonic acid equivalent for 'Avrolles'; 0, 0.03, 0.06, 0.24, 0.94, 3.75, 15 and 30 mmol/L galacturonic acid equivalent for 'Marie Ménard')

were prepared along the lines and columns, respectively. Solutions were prepared in citrate/phosphate buffer at pH 3.8, 0.1 M ionic strength. Equal amounts (50 µL) of pectins and procyanidins solutions were mixed and stirred for 20 s before each measurement. Controls were a line or column containing only procyanidins or pectins in buffer. After spectra were collected, microplates were centrifuged 10 min at 2100 x *g*. Supernatants of control wells (pectins at 15/30 mmol/L in buffer, named S1A) and (procyanidins at a concentration of 30/60 mmol/L, named S1B) and supernatants of wells containing procyanidins at a concentration of 30/60 mmol/L with pectin at a concentration of 15/30 mmol/L (named S2) were analyzed using High-Performance Liquid Chromatography with Diode Array Detection (HPLC-DAD) and High Performance Size-exclusion Chromatography coupled with Multi-Angle Laser Light Scattering (HPSEC-MALLS). (ΔM_w = S2−S1A) and (ΔDP_n = S2−S1B) were used to define qualitative changes in weight-average molar mass of pectins and in number average degree of polymerization of procyanidins, respectively.

2.6. Isothermal Titration Calorimetry (ITC)

The entropy and enthalpy changes caused by the interactions between procyanidins and pectins were determined by ITC, using TAM III microcalorimeter (TA instruments, New Castle, USA). Purified procyanidins (60 mmol/L in (-)-epicatechin equivalent) and pectins (7.5 mmol/L galacturonic acid equivalent) were dissolved in the same citrate/phosphate buffer pH 3.8, 0.1 M ionic strength. The reference cell was filled by water. All solutions were degassed prior to measurements. The pectin solution was placed in the 850 mL sample cell of the calorimeter and the

procyanidin solution was loaded into the injection syringe and titrated into the sample cell by 50 injections of 5 μL. Each injection lasted 5 s, with separating delay of 20 min. The content of the sample cell was stirred throughout the experiment at 90 rev/min. The raw ITC data as a plot of heat flow (microjoules per second) against time (minutes) were then integrated peak-by peak and normalized to obtain a plot of observed enthalpy change per mole of injectant (ΔH, kJ/mol) against the molar ratio (epicatechin/galacturonic acid). Peak integration was performed and the experimental data were fitted to a theoretical titration curve using the instrument software (NanoAnalyze 3.10.0). Control experiments include the titration of procyanidin fractions into buffer and are subtracted from titration experiments. The thermodynamic parameters including binding stoichiometry (n), binding constant (K_a), enthalpy (ΔH) and entropy (ΔS), the 'S' shape curve as adjustable parameters. Experiments were carried out in duplicates.

2.7. Statistical analysis

Results were expressed as mean values, and their reproducibility was presented as the pooled standard deviation (Pooled SD). For each series of repeated samples, the pooled SDs were calculated using the sum of their respective variances multiplied by their respective degrees of freedom (Box, Hunter, & Hunter, 1978). Principal Component Analysis (PCA) was realized using the functions of the library FactoMineR and Factoextra in R statistical software (R Core Team., 2014). Heatmap was performed with Python 3.5 software using the Seaborn package (Waskom, 2014).

3. Results

3.1. Structure and composition of fractions

3.1.1. Procyanidins

The two apple varieties ‘Marie Ménard’ and ‘Avrolles’ were chosen to obtain two purified fractions of intermediate and high degree of polymerization, respectively (Le Bourvellec, Guyot, & Renard, 2009). The composition of isolated apple phenolic fractions is shown in Table 1. The purified extracts from ‘Marie Ménard’ and ‘Avrolles’ contained ca. 700 mg/g of polyphenols, mainly procyanidins plus traces of flavan-3-ol monomer i.e. (-)-epicatechin, hydroxycinnamic acids, i.e. 5′-caffeoylquinic acid and *p*-coumaroylquinic acid, dihydrochalcones, i.e. phloretin xyloglucoside and phloridzine, and a mix of flavonols. ‘Marie Ménard’ and ‘Avrolles’ procyanidins were characterized by $\overline{DP}n$ = 9 and 79, respectively. Both were constituted by more than 98 % (-)-epicatechin units and contained a homologous structure differing by their degree of polymerization. All the results were consistent with Le Bourvellec et al. (2004) and (2012).

3.1.2. Pectins

Detailed compositions of the pectins are available in Liu et al. (2021) and the sugar ratios based on the sugar content and macromolecular characteristic for pectins are calculated in Table 1. HPSEC chromatograms and molar mass distributions of the pectins are presented in Fig. 1. Structural diversity was obtained on two major parameters, namely (i) the nature and composition of side-chains and (ii)

macromolecular characteristics, which varied independently in this series of pectins (as described by principal component analysis loading and sample plots in Supplementary Fig. 1). Concerning the neutral sugar side chain abundance and composition, apple pectins were characterized by high xylose, signaling presence of xylogalacturonans (Schols, Bakx, Schipper, & Voragen, 1995). Only beet pectins contained detectable ferulic acid, and they had the highest content of neutral sugars, notably arabinose, and highest degree of acetylation. Kiwifruit pectins appeared to be the richest in homogalacturonans, with the lowest arabinose content and arabinose to galactose ratio. All these characteristics were further modulated by the pH used for pectin solubilization, with pectins solubilized at pH 2.0 displaying the most extreme characteristics for their respective origins. Unsaturated double bonds resulting from β-elimination have been detected in AP6, BP6, KPR6 and KPO6 (Liu et al., 2021), leading to reduction of the HG chain length and its potential binding sites after pH 6.0 treatment.

Further information on pectin conformations in solution, calculated by plotting the molar mass versus the intrinsic viscosity obtained with HPSEC-MALLS, is given in Table 2. Two regions were used to determine the Mark-Houwink-Sakurada conformation parameters at different peaks. In the main peak, the exponent α varied between 0.96 and 1.32 indicating an organization close to stiff coils in a good solvent (Flory, 1953), with various chain flexibility in agreement with literature data (Fishman, Chau, Kolpak, & Brady, 2001), excepted for AP2 ($\alpha = 0.55$) which exhibited a value corresponding to random coil conformation in a θ solvent. Most

pectins (except AP2) also presented a less important fraction (generally shoulder in the chromatogram from 20 – 23 mL, Fig. 1) exhibiting a spheroidal or denser conformation (Table 2) (α between 0 and 0.41) that could correspond to branched aggregates or more folded conformation (Alba, Bingham, Gunning, Wilde, & Kontogiorgos, 2018; Lopez-Torrez, Nigen, Williams, Doco, & Sanchez, 2015). This minor fraction represented a higher proportion in AP6 and KPRs (Fig. 1) and seemed to correspond to the main peak in AP2. The lower values of the exponent α (0.55) thus obtained for the main peak in AP2 could be due to a more folded molecule, and this intermediate value (between the sphere and the rod) was most probably caused by the presence of two populations under the main peak, which produced artificially one lower exponent instead of two exponents. Meanwhile, the population of these peaks will undergo some modifications after interaction with procyanidins. Detailed information will be given in the interaction section.

Good diversities and variabilities were obtained in this sample set for pectin linearity, length of side chains, arabinans / galactans ratio, degree of acetylation, molar mass and conformation. No pectins with a low degree of methylation (DM < 30) were present. This should not affect the investigation of the subsequent interactions as it has been proved that the affinity of low methylated pectins to procyanidins is very low (Watrelot et al., 2013).

3.2. Interactions with procyanidins of DP9

3.2.1. Isothermal titration calorimetry

Thermodynamic parameters from ITC titration of pectins by procyanidins DP9 are shown in Table 3A. Typical thermograms were obtained for AP2/3, BP2, KPR2/3/6 and KPO2 (7.5 mM galacturonic acid equivalent) titrated by procyanidin DP9 (60 mM (-)-epicatechin equivalent) with strong exothermic peaks (data not shown). In contrast, no titration could be observed for AP6, BP3/6 and KPO3/6 by procyanidin DP9. Stoichiometry (defined as ratio of (-)-epicatechin/galacturonic acid) was ca. 0.1 for AP2/3, BP2 and KPO2 (1 molecule of (-)-epicatechin bound 10 units of galacturonic acid) and ca. 0.14 for KPR2 (1 molecule of (-)-epicatechin bound 7 units of galacturonic acid) using a one-site model.

The association constant ranged between 2.0×10^3 M^{-1} and 1.2×10^4 M^{-1} and increased in the following order: AP3 ≈ BP2 < KPR3 ≈ KPR6 ≈AP2 << KPR2 <<< KPO2 (Table 3A). KPO2 with the highest Gal A/Rha ratio (91) had the highest affinity for procyanidin DP9, showing a strong positive impact of pectin linearity on their ability to interact with procyanidins. Analysis of the thermodynamic contributions ($\Delta G = \Delta H - T\Delta S$) related to the exothermic reactions indicated a strong entropy contribution ($-T\Delta S$ from -18 to -14 kJ/mol) showing that the interactions were mostly driven by entropy, i.e. by hydrophobic interactions and the release of water molecules (Le Bourvellec & Renard, 2012; Poncet-Legrand, Gautier, Cheynier, & Imberty, 2007; Watrelot et al., 2013, 2014). The enthalpy contributions were very limited for AP3, AP2 and KPR3 (ΔH from -1 to -4 kJ/mol) and higher for AP2, KPR2/6 and KPO2 (ΔH from -6 to -5 kJ/mol) indicating that interactions also involved hydrogen bonds. The proportion of enthalpy for KPR/Os was significantly

379 higher than that of AP3 and BP2 (Table 3A) due to hydrogen bonds which increased
380 their affinity for procyanidin DP9.

381 **3.2.2. Phase diagram**

382 Fig. 2A, B present the heat-map of turbidity at 650 nm. Turbidity of all pectin
383 mixtures with procyanidins DP9 rose with increasing pectin concentrations (Fig. 2A).
384 This increase was more marked at 30 mM galacturonic acid equivalent for KPR2 and
385 KPO2, with absorbance values of 1.03 and 0.92, respectively, than for other pectins
386 (absorbance from 0.21 to 0.48) at the same concentration. These results were
387 consistent with the results of ITC. The interactions between highly linear pectins and
388 procyanidin DP9 led to formation of aggregates with marked turbidity. For APs,
389 BP3/6, KPR2/3 and KPO2/3, the absorbances at 650 nm increased slightly at a
390 concentration of 30 mM galacturonic acid equivalent. After 3.75 mM pectin
391 concentration, the absorbance of BP2 stabilized around at 0.2. However, AP6, BP3/6
392 and KPO3/6 also showed increased turbidity while no interactions had been detected
393 by ITC. This result may indicate that the resulting released or absorbed heat during
394 the interaction stayed below the limit of detection of the nanocalorimetric method.
395 Absorbance of all pectins at 30 mM (-)-galacturonic acids equivalent rose with
396 increased procyanidins DP9 concentrations (Fig. 2B), which was consistent with the
397 trend of Fig. 2A.

398 **3.2.3. Characterization of unbound pectin and procyanidins**

399 The free pectins and procyanidins remaining in the wells after interactions with

30 mM galacturonic acid and 60 mM (-)-epicatechin equivalents were investigated to further understand the impact of the interactions on their macromolecular structure (Fig. 1, Table 4). Fig. 1 showed the chromatograms obtained by HPSEC-MALLS of the initial pectic compounds in buffer (S1A) and the free pectin compounds (at 30 mM in galacturonic acid equivalent) after binding with procyanidins (S2, i.e. pectic compounds that had not formed aggregates). Table 4 showed the corresponding pectin macromolecular characteristics.

After interaction, only 2% -5% of pectins remained in the supernatant. More pectin remained free for AP6, BP6 and KPO/R6 than for AP2/3, BP2/3 and KPO/R2/3, respectively (Table 4). On the one hand, the $\overline{M}_w$ of free pectins after binding with procyanidins was lower than the $\overline{M}_w$ of initial pectin sample (Table 4). Procyanidin DP9 may have strong selectivity for the bigger molecules of pectin fractions, especially AP2 (ΔM_w: -266), KPR2 (ΔM_w: -216) and KPR3 (ΔM_w: -223). On the other hand, the $\overline{DP}n$ of free procyanidins after interaction with pectins was lower than the $\overline{DP}n$ of initial procyanidin sample, whatever pHs and species (Table 4), confirming that pectins preferentially interacted with highly polymerized procyanidins.

In comparison with the initial pectin solutions, the main peaks of free APs, BPs, KPRs and KPOs in the solutions slightly shifted to higher elution volumes indicating a decrease in hydrodynamic volume (Fig. 1). Moreover, the shoulder at a lower elution time (corresponding to the high molar mass fraction) in the main peak of AP6 and KPR/Os decreased after interaction due to complexation with procyanidins. The

molecules that remained in supernatants after pectin-procyanidin interactions were smaller procyanidins DP9 and smaller pectins. The large-sized pectins and the larger procyanidins were co-aggregated, or the aggregates contained procyanidins of higher $\overline{DP}n$ and pectins with larger hydrodynamic volume. Nevertheless, it was challenging to use the α value obtained from Mark-Houwink-Sakurada equation to determine which pectin conformation was more conducive to interaction as this value did not show clear trend probably because it only provided some general structural information on these pectins (Table 2).

3.3. Interactions with procyanidins of DP79

3.3.1. Isothermal titration calorimetry

Titration of all pectins by procyanidins DP79 showed complex curves characterized by strong exothermic peaks. Thermodynamic parameters are shown in Table 3B. Stoichiometry (n) results, suggested that approximately 1 (-)-epicatechin constitutive unit bound to 5 units of galacturonic acid for high linearity KPO2. For AP3, KPR3/6 and KPO3/6 with medium linearity, approximately 1 (-)-epicatechin constitutive unit bound to 10 units of galacturonic acid. While, the stoichiometry for AP2 with high molar mass and size, and BP2/3 with high arabinans side chains were ca. 0.5.

The association constant K_a between pectins and procyanidins DP79 ranged from 0.3 × 10^2 M^{-1} to 1.2 × 10^4 M^{-1} in the order BP2 ≈ BP3 ≈ BP6 <<KPR3 <KPR6 <AP6 <AP3 <<AP2 <KPO3 < KPO6 << KPR2 < KPO2. In particular, the BP2, AP2,

KPR2 and KPO2 pectins were the most different from our sample set (Supplementary Fig. 1) and cover a wide range of affinity. Regarding the interactions between all pectins and procyanidins DP79, contribution of entropy (-TΔS from -12 to -19 kJ/mol) related to the exothermic reactions, indicated that the interactions were mostly driven by entropy indicating hydrophobic interactions and water released. Moreover, an enthalpy contribution especially for KPR2 (ΔH = - 6.0 kJ/mol) and KPO2 (ΔH = - 8.0 kJ/mol) was also observed indicating that hydrogen bonds were also involved.

3.3.2. Phase diagram

More precipitation was obtained with procyanidins of DP79 (Fig 3. A, B) than of DP 9, regardless of pectin type. Turbidity increased dramatically with the increase of concentration of galacturonic acid and procyanidins for AP2, BP2, KPR2 and KPO2, indicating strong interactions, which confirmed the result of ITC. The turbidity for AP2, BP2, KPR2 and KPO2 with procyanidins DP79 at 15 mM galacturonic acid equivalent or 30 mM (-)-epicatechin equivalent increased in the following the order: KPO6 < KPR6 <AP6 < KPR3 ≈ BP2 < AP2 < BP3<BP6 <KPO3<KPR2 <AP3 <KPO2.

3.3.3. Characterization of unbound pectin and procyanidins

After interactions between pectins (30 mM galacturonic acid equivalent) and procyanidin DP79 (60 mM epicatechin equivalent), 4% - 11% of the pectins remained in the supernatants (Table 4). Similarly, more pectins remained in solution for AP6, BP6 and KPO/R6 than for AP2/3, BP2/3 and KPO/R2/3, respectively. $\overline{M}_w$ of all

pectins and $\overline{DP}n$ of procyanidin DP79 obviously decreased after interactions (Table 4). The ΔM_w obtained between APs, BPs, KPR/Os and procyanidins DP79 were higher than the ones obtained with procyanidin DP9, especially for AP2. Procyanidin DP79 gave a higher ΔDP_n for all pectins ranging from - 56 to - 38. This high decrease of the degree of polymerization and molar mass indicated that highly polymerized procyanidins of fraction DP79 associated selectively with pectins of higher molar mass. HPSEC-MALLS chromatograms of the pectins also support this conclusion. Like with procyanidin DP9, the main population of free APs, BPs, KPRs and KPOs was slightly shifted to lower sizes after complexation/aggregation and the largest population disappeared (Fig. 3). This suggested that the large-sized pectin aggregates from the largest population preferentially interact with large-sized procyanidins DP79 and produce precipitates (Alba et al., 2018; Carn et al., 2012). However, this specificity can not be distinguished in different conformations of pectins, because α values of large populations are all in the range of 0 - 0.41 representing large-sized folded structures or branched aggregates did not show clear trend (Table 2).

4. Discussion

4.1. Comparison of calorimetry and turbidity methods

Using both isothermal titration calorimetry and turbidity, pectins with different linearity (or side-chain abundance) and macromolecular characteristics were shown to interact with procyanidins (DP9 and DP79). These interactions were mainly driven by entropy, which may be caused by hydrophobic interactions, or changes in solvation and conformation (Leavitt & Freire, 2001; Poncet-Legrand et al., 2007). Enthalpy

contributions were also observed indicating that interactions also involved some hydrogen bonds. Haze formation was observed for all pectins with procyanidins DP9, while for some pectin fractions, AP6, BP3/6, and KPO3/6, the interactions were below the detection limit for nano calorimetry. The reason may be that the ITC signal generated by these pectin-procyanidin interactions (exothermic) is masked by the concurrent endothermic signal from chain-chain interaction during pectin aggregation. In addition, the pectins for which no titration could be detected were generally characterized by higher arabinose contents: although procyanidins do interact with arabinans (Fernandes et al., 2020), this polymer appeared to lead to less intense binding. This was not observed with procyanidins DP79, which had higher energies of interactions and generally higher affinities than DP9. Turbidity appeared to be more sensitive than ITC for detection of interactions. Haze formation is a complex process which involves the modification of intra-molecular and molecule-solvent interactions. A limit to measuring turbidity however is that it must be observed under static conditions, and the lack of stirring during the complete measurement may result in uneven cloudiness / aggregate formation (Watrelot, Renard, & Le Bourvellec, 2015). Moreover, procyanidins, and notably the larger procyanidins, can auto-aggregate (Carn et al., 2012) and their sedimentation increased with $\overline{DP}n$. The turbidity measurement provided information on the formation of insoluble complexes, but it cannot provide information on the mechanism and binding sites. These two methods are complementary, allowing higher sensitivity for detection of the interactions (haze formation) on the one hand and access to stoichiometric ratio and binding enthalpy

508 (ITC) on the other hand.

509 **4.2. Pectin linearity**

510 The highest affinities for procyanidins DP9/79 were obtained for kiwifruit pectins
511 KPO2 and KPR2, with both the highest K_a and the most marked aggregate formation,
512 and the lowest affinities were observed for beet pectins. KPR/Os exhibited the highest
513 linearity, HG and galactans contents, and lower RG-I content (Table 1 and
514 Supplementary Fig. 1). Ripening involves a decrease in arabinose and a loss of pectic
515 side chains (Liu et al., 2021) resulting in even higher linearity and higher HG ratio in
516 KPO2, which strengthen the binding to procyanidins. Brahem et al. (2019) also
517 reported that cell walls from pear at an overripe stage have a higher affinity for
518 procyanidins than those from the ripe stage, due to removal of arabinan and galactan
519 pectin side chains during ripening, allowing better access to galacturonic acid-rich
520 molecules. Moreover, the adsorption of anthocyanins on blueberry linear
521 chelator-soluble pectins is four times higher than on the highly branched
522 water-soluble pectin (Koh, Xu, & Wicker, 2020). On the other hand, Watrelot et al.
523 (2014) described that the affinity of procyanidin DP30 to pectic compounds increases
524 in the following order: arabinans < arabinans + galactans II < galactan I . This may be
525 due to the length and the flexibility of galactan side chains, while arabino-galactan
526 side chains are short, more branched and stiff (M'sakni et al., 2006). Highly branched
527 arabinans have more globular structures which limit their interactions with
528 polyphenols (Fernandes et al., 2020). KPR/Os contained more galactan side chains,
529 while BPs contained more arabinans, followed by APs. Therefore, structure of the

side-chains may also have contributed to the higher affinity of KPR/Os for procyanidins DP79. Interactions between BPs and procyanidin DP79 showed association constants of the order of 10^2 M^{-1}. The differences in affinity constants between the different pH fractions were very limited, ranging between 0.3 × 10^2 M^{-1} (BP2) and 0.4 × 10^2 M^{-1} (BP3/6). The low affinity performance of BPs may be not only due to their complex arabinan side chain structures, but also to the presence of ferulic acid covalently linked to arabinans, and to their acetylation. Ferulic acid cross-linking, by further rigidifying the arabinan side-chains, might lower interactions with procyanidins due to steric hindrance. This is consistent with Fernandes et al. (2020) who reported that the branched arabinan side chains in pectin limit their interactions with polyphenols.

4.3. Impact of pectins molar mass on interactions

AP2, with higher molar mass, intrinsic viscosity, hydrodynamic radius and lower density, had higher affinity for procyanidin DP9/79 than AP3 and AP6; this was also true when comparing KPR2 or KPO2 to KPR3/6 and KPO3/6. This was the same relation as with corn silk polysaccharides, for which the binding capacity to flavonoids increases with molar mass (Guo, Ma, Xue, Gao, & Chen, 2018). However, this relationship only appeared true within a series with otherwise similar structural features, as KPR2 and KPO2 had lower molar masses but higher affinities than AP2. This suggests that increasing the molar mass of pectins alone may not increase their adsorption capacity. The linear structure of pectins was more important than their molar mass for binding to procyanidins.

552 Higher molar mass pectins have more glycosidic bonds, therefore more potential
553 binding sites, which contribute to the adsorption of polyphenols. Moreover, a larger
554 hydrodynamic radius and lower density may also mean that there was more space for
555 procyanidins to interact with the polysaccharide molecule. Meanwhile, a larger space
556 for bending and turning, a larger effective volume, a larger flow resistance, and a
557 higher frequency of collisions between segments produce high intrinsic viscosity
558 (BeMiller & Whistler, 1996). Pectins with higher intrinsic viscosity, that is existing as
559 expanded chains in solution, might better interact with procyanidins (Fig. 4A). In
560 addition, most carboxyl groups in pectins are ionized when the pH is higher than their
561 pKa, which was the case in the experiments (pH 3.8 > pKa 3.5). This ionization leads
562 to coulomb repulsion between the consecutive free carboxyls on a pectin molecule,
563 increasing its stiffness (Stoddart, Spires, & Tipton, 1969), and preventing spatial
564 proximity between segments of two pectin molecules (Fig. 4B). This causes the chain
565 to stretch, which may result in more space to adsorption.

566 **4.4. Substitution of the galacturonic acids**

567 The DM of pectin has already been demonstrated to be a very important factor for
568 interactions. However, all the pectins used here had high degrees of methylation (>
569 70), allowing strong interactions with procyanidins (Watrelot et al. (2013). Although
570 KPR/Os were less methylated than APs and BPs, they still had a high DM (> 73),
571 which did not limit their high affinity for procyanidins. Moreover, the intensity of the
572 interaction seems to decrease with increasing acetylation. KPR/Os have the lowest
573 degree of acetylation with a high affinity for procyanidins, while BPs have the highest

574 degree of acetylation with the lowest affinity. However, a simple comparison may be
575 misleading as there are confounding factors which should be considered, e.g., pectin
576 linearity.

577 We noted that the overall enthalpy of interactions with KPR/Os were significantly
578 higher than with APs and BPs, especially KPR/O2 (Table 3), suggesting more
579 hydrogen bonds. Most previous studies focused on commercial pectin (usually not
580 acetylated and sometimes demethylated), purified HG or RG. Watrelot et al. (2013)
581 reported that interactions between commercial apple and citrus pectins and
582 procyanidins is also mostly driven by entropy. However, the interactions between
583 rhamnogalacturonans and hairy regions of pectins and procyanidins could be driven
584 by either enthalpy or entropy or both (Watrelot et al., 2014). Similarly, the interactions
585 between apple pectins extracted at pH 3.8 (from 'Ariane' cultivar) and procyanidins
586 (DP9) are entropy-driven (Le Bourvellec et al., 2012). Most pectin-procyanidin
587 interactions are driven by both entropy and enthalpy, but their proportions may be
588 regulated by the degree of esterification of pectins.

589 **4.5. Degree of polymerization of procyanidins**

590 As expected, the interactions were higher with the procyanidins of the highest
591 degree of polymerization. With procyanidins DP79, marked aggregation appeared for
592 all pectin fractions (absorbance > 0.9) at the maximum concentration of both, while
593 with procyanidins DP9 formation of cloud or aggregate were relatively lower.
594 However, two trends were observed for ITC results. APs, BP3/6, KPR2 and KPRs had
595 a higher affinity with DP79 than DP9 by ITC, but BP2 and KPR3/6 had a lower

affinity with DP79 than DP9, especially BP2, the affinity of which was lower by one order of magnitude. This may be due to the conformational constraints of the two molecules that limit their interactions with each other. BP2 had low pectin linearity and HG content, together with the highest neutral sugar side-chains content of the twelve pectins, especially arabinans, and high ferulic acid content. On the one hand, these structures might cross-link the chains and limit the available binding sites for complexation with procyanidins. On the other hand, procyanidins DP79 may exhibit longer length and larger size, and are less uniform than procyanidins DP30 and DP9. Using the Fisher-Burford model to fit the SAXS spectrum, Vernhet, Carrillo, & Poncet-Legrand (2014) reported that the apple proanthocyanidins of DP69 and DP80 have a more dense shape with branches. Zanchi et al. (2009) described polymeric proanthocyanidins containing about 6% ramifications. Therefore, high DP procyanidins may induce intramolecular hydrophobic interactions and hydrogen bonds resulting in more aggregated and less extended structure. Watrelot et al. (2013, 2014) showed that pectins interact preferentially with highly polymerized procyanidins DP30, and that structure and size of procyanidins DP30 facilitates aggregates formation. Using larger procyanidins facilitated detection of the selectivity of various pectins, DP79 being less favorable with some specific structures due to its conformation.

Each polysaccharide has its own unique chemical composition, structure, molecular architecture or conformation, and these factors interact with each other to influence their adsorption to procyanidins. The interaction between these factors

618 remains complex, and more work will be needed to clarify their internal relationship.

619 **5. Conclusions**

620 Procyanidins showed different binding selectivity to apple, beet and kiwifruit
621 pectins depending on the compositions and macromolecular features of the pectins
622 and degree of polymerization of procyanidins. High molar mass and low density
623 contributed to procyanidin adsorption. Pectins with high linearity and HG content,
624 and low arabinan branching had highest interaction with procyanidins. On the
625 contrary, high RG-I branching and ferulic acid content limited the affinity to
626 procyanidins. Higher number average DP of procyanidins might hinder the adsorption
627 of pectins with high side chain branching. The importance of factors affecting pectin
628 selectivity were linearity (proportion of side-chains) > molar mass > density ≈
629 hydrodynamic radius, with high branching and density being detrimental to
630 interaction while high molar mass was favorable. Combining different factors,
631 capacity of association between procyanidin DP79 and pectins could be ranked:
632 KPO2 > KPR2 > AP2 > BP2 (Fig. 5).

633 Consequently, a deep understanding of various processing-structures-binding
634 capacity of pectins to procyanidins aids food workers customize the functional
635 characteristics of plant-derived products and provide effective guidance for processing.
636 Systematic variation of pectin structural features thus allows to better understand
637 polyphenol affinity and may pave the way to anticipate the variability of retention of
638 polyphenols in different fruits and vegetables.

Acknowledgements

LIU Xuwei would like to acknowledge China Scholarship Council (CSC) and Institut National de Recherche pour l'Agriculture, l'Alimentation, et l'Environnement (INRAE) for financial support to his PhD study. The authors thank the various CPER Platform 3A funders for the support to the HPSEC-MALLS measures as well as the related financial support from the European Union with the European Regional Development Fund, the State, the Provence-Alpes-Côte d'Azur Region, the Departmental Council of Vaucluse and the Urban Community of Greater Avignon.

References

Alba, K., Bingham, R. J., Gunning, P. A., Wilde, P. J., & Kontogiorgos, V. (2018). Pectin Conformation in Solution. *Journal of Physical Chemistry B*, *122*(29), 7286–7294. https://doi.org/10.1021/acs.jpcb.8b04790

BeMiller, J. N., & Whistler, R. L. (1996). Carbohydrates. In O. R. Fennema. (Ed.), *Food Chemistry* (pp. 157–225). New York: Marcel Dekker.

Box, G. E., Hunter, W. G., & Hunter, J. S. (1978). *Statistics for Experimenters, an Introduction to Design, Data Analysis and Model Building*. *New-York, Wiley and Sons*.

Brahem, M., Renard, C. M. G. C., Bureau, S., Watrelot, A. A., & Le Bourvellec, C. (2019). Pear ripeness and tissue type impact procyanidin-cell wall interactions. *Food Chemistry*, *275*, 754–762. https://doi.org/10.1016/j.foodchem.2018.09.156

Caffall, K. H., & Mohnen, D. (2009). The structure, function, and biosynthesis of plant cell wall pectic polysaccharides. *Carbohydrate Research*, *344*(14), 1879–1900. https://doi.org/10.1016/j.carres.2009.05.021

Carn, F., Guyot, S., Baron, A., Pérez, J., Buhler, E., & Zanchi, D. (2012). Structural properties of colloidal complexes between condensed tannins and polysaccharide hyaluronan. *Biomacromolecules*, *13*(3), 751–759. https://doi.org/10.1021/bm201674n

Dobson, C. C., Mottawea, W., Rodrigue, A., Buzati Pereira, B. L., Hammami, R., Power, K. A., & Bordenave, N. (2019). Impact of molecular interactions with phenolic compounds on food polysaccharides functionality. In I. C. F. R. Ferreira & L. Barros (Eds.), *Advances in Food and Nutrition Research* (Vol. 90, pp. 135–181). Elsevier Inc. https://doi.org/10.1016/bs.afnr.2019.02.010

Dongowski, G. (2001). Enzymatic degradation studies of pectin and cellulose from red beets. *Nahrung - Food*, *45*(5), 324–331. https://doi.org/10.1002/1521-3803(20011001)45:5<324::AID-FOOD324>3.0.CO;2-C

Einstein, A. (1906). Eine neue Bestimmung der Moleküldimensionen. *Annalen Der*

Physik, *324*(2), 289–306.

Einstein, A. (1911). Berichtigung zu meiner Arbeit: Eine neue Bestimmung der Moleküldimensionen" . *Annalen Der Physik*, *339*(3), 591–592.

Fernandes, P. A. R., Le Bourvellec, C., Renard, C. M. G. C., Wessel, D. F., Cardoso, S. M., & Coimbra, M. A. (2020). Interactions of arabinan-rich pectic polysaccharides with polyphenols. *Carbohydrate Polymers*, *230*, 115–644. https://doi.org/10.1016/j.carbpol.2019.115644

Fishman, M. L., Chau, H. K., Kolpak, F., & Brady, J. (2001). Solvent effects on the molecular properties of pectins. *Journal of Agricultural and Food Chemistry*, *49*(9), 4494–4501. https://doi.org/10.1021/jf001317l

Flory, P. J. (1953). Molecular configuration of polyelectrolytes. *The Journal of Chemical Physics*, *21*(1), 162–163.

Fraeye, I., De Roeck, A., Duvetter, T., Verlent, I., Hendrickx, M., & Van Loey, A. (2007). Influence of pectin properties and processing conditions on thermal pectin degradation. *Food Chemistry*, *105*(2), 555–563. https://doi.org/10.1016/j.foodchem.2007.04.009

Guo, Q., Ma, Q., Xue, Z., Gao, X., & Chen, H. (2018). Studies on the binding characteristics of three polysaccharides with different molecular weight and flavonoids from corn silk (Maydis stigma). *Carbohydrate Polymers*, *198*, 581–588. https://doi.org/10.1016/j.carbpol.2018.06.120

Guyot, S., Marnet, N., & Drilleau, J. F. (2001). Thiolysis - HPLC characterization of apple procyanidins covering a large range of polymerization states. *Journal of Agricultural and Food Chemistry*, *49*(1), 14–20. https://doi.org/10.1021/jf000814z

Janaswamy, S., & Chandrasekaran, R. (2005). Polysaccharide structures from powder diffraction data: Molecular models of arabinan. *Carbohydrate Research*, *340*(5), 835–839. https://doi.org/10.1016/j.carres.2004.12.035

Jin, W., Xiang, L., Peng, D., Liu, G., He, J., Cheng, S., … Huang, Q. (2020). Study on the coupling progress of thermo-induced anthocyanins degradation and

polysaccharides gelation. *Food Hydrocolloids*, *105*, 105822. https://doi.org/10.1016/j.foodhyd.2020.105822

Kardum, N., & Glibetic, M. (2018). Polyphenols and their interactions with other dietary compounds: implications for human health. In *Advances in Food and Nutrition Research* (Vol. 84, pp. 103–144). Elsevier Inc. https://doi.org/10.1016/bs.afnr.2017.12.001

Koh, J., Xu, Z., & Wicker, L. (2020). Binding kinetics of blueberry pectin-anthocyanins and stabilization by non-covalent interactions. *Food Hydrocolloids*, *99*, 105–354. https://doi.org/10.1016/j.foodhyd.2019.105354

Le Bourvellec, C., Boas, P. B. V., Lepercq, P., Comtet-Marre, S., Auffret, P., Ruiz, P., … Mosoni, P. (2019). Procyanidin—cell wall interactions within apple matrices decrease the metabolization of procyanidins by the human gut microbiota and the anti-inflammatory effect of the resulting microbial metabolome in vitro. *Nutrients*, *11*(3), 664. https://doi.org/10.3390/nu11030664

Le Bourvellec, C., Bouzerzour, K., Ginies, C., Regis, S., Plé, Y., & Renard, C. M. G. C. (2011). Phenolic and polysaccharidic composition of applesauce is close to that of apple flesh. *Journal of Food Composition and Analysis*, *24*(4–5), 537–547. https://doi.org/10.1016/j.jfca.2010.12.012

Le Bourvellec, C., Guyot, S., & Renard, C. M. G. C. (2004). Non-covalent interaction between procyanidins and apple cell wall material: Part I. Effect of some environmental parameters. *Biochimica et Biophysica Acta - General Subjects*, *1672*(3), 192–202. https://doi.org/10.1016/j.bbagen.2004.04.001

Le Bourvellec, C., Guyot, S., & Renard, C. M. G. C. (2009). Interactions between apple (Malus x domestica Borkh.) polyphenols and cell walls modulate the extractability of polysaccharides. *Carbohydrate Polymers*, *75*(2), 251–261. https://doi.org/10.1016/j.carbpol.2008.07.010

Le Bourvellec, C., & Renard, C. M. G. C. (2005). Non-covalent interaction between procyanidins and apple cell wall material. Part II: Quantification and impact of cell wall drying. *Biochimica et Biophysica Acta - General Subjects*, *1725*(1), 1–9.

https://doi.org/10.1016/j.bbagen.2005.06.003

Le Bourvellec, C., & Renard, C. M. G. C. (2012). Interactions between polyphenols and macromolecules: Quantification methods and mechanisms. *Critical Reviews in Food Science and Nutrition*, *52*(3), 213–248. https://doi.org/10.1080/10408398.2010.499808

Le Bourvellec, C., & Renard, C. M. G. C. (2019). Interactions between polyphenols and macromolecules: Effect of tannin structure. In L. Melton, F. Shahidi, & P. Varelis (Eds.), *Encyclopedia of Food Chemistry* (pp. 515–521). Elsevier. https://doi.org/10.1016/B978-0-08-100596-5.21486-8

Le Bourvellec, C., Watrelot, A. A., Ginies, C., Imberty, A., & Renard, C. M. G. C. (2012). Impact of processing on the noncovalent interactions between procyanidin and apple cell wall. *Journal of Agricultural and Food Chemistry*, *60*(37), 9484–9494. https://doi.org/10.1021/jf3015975

Leavitt, S., & Freire, E. (2001). Direct measurement of protein binding energetics by isothermal titration calorimetry. *Current Opinion in Structural Biology*, *11*(5), 560–566. https://doi.org/10.1016/S0959-440X(00)00248-7

Li, X., Liu, G., Tu, Y., Li, J., & Yan, S. (2019). Ferulic acid pretreatment alleviates the decrease in hardness of cooked Chinese radish (Raphanus sativus L. var. longipinnatus Bailey). *Food Chemistry*, *278*, 502–508. https://doi.org/10.1016/j.foodchem.2018.10.086

Liu, X., Le Bourvellec, C., & Renard, M. G. C. C. (2020). Interactions between cell wall polysaccharides and polyphenols: Effect of molecular internal structure. *Comprehensive Reviews in Food Science and Food Safety*. https://doi.org/10.1111/1541-4337.12632

Liu, X., Renard, C. M. G. C., Rolland-Sabaté, A., Bureau, S., & Le Bourvellec, C. (2021). Modification of apple, beet and kiwifruit cell walls by boiling in acid conditions: common and specific responses. *Food Hydrocolloids*, *112*, 106266. https://doi.org/10.1016/j.foodhyd.2020.106266

Loo, Y. T., Howell, K., Chan, M., Zhang, P., & Ng, K. (2020). Modulation of the

human gut microbiota by phenolics and phenolic fiber-rich foods. *Comprehensive Reviews in Food Science and Food Safety*, *19*(4), 1268–1298. https://doi.org/10.1111/1541-4337.12563

Lopez-Torrez, L., Nigen, M., Williams, P., Doco, T., & Sanchez, C. (2015). Acacia senegal vs. Acacia seyal gums - Part 1: Composition andstructure of hyperbranched plant exudates. *Food Hydrocolloids*, *51*, 41–53. https://doi.org/10.1016/j.foodhyd.2015.04.019

M'sakni, N. H., Majdoub, H., Roudesli, S., Picton, L., Le Cerf, D., Rihouey, C., & Morvan, C. (2006). Composition, structure and solution properties of polysaccharides extracted from leaves of Mesembryanthenum crystallinum. *European Polymer Journal*, *42*(4), 786–795. https://doi.org/10.1016/j.eurpolymj.2005.09.014

Mamet, T., Ge, Z. zhen, Zhang, Y., & Li, C. mei. (2018). Interactions between highly galloylated persimmon tannins and pectins. *International Journal of Biological Macromolecules*, *106*, 410–417. https://doi.org/10.1016/j.ijbiomac.2017.08.039

McManus, J. P., Davis, K. G., Beart, J. E., Gaffney, S. H., Lilley, T. H., & Haslam, E. (1985). Polyphenol interactions. Part 1. Introduction; some observations on the reversible complexation of polyphenols with proteins and polysaccharides. *Journal of the Chemical Society, Perkin Transactions 2*, *28*(9), 1429. https://doi.org/10.1039/p29850001429

Mohnen, D. (2008). Pectin structure and biosynthesis. *Current Opinion in Plant Biology*, *11*(3), 266–277. https://doi.org/10.1016/j.pbi.2008.03.006

Monfoulet, L.-E., Buffière, C., Istas, G., Dufour, C., Le Bourvellec, C., Mercier, S., … Morand, C. (2020). Effects of the apple matrix on the postprandial bioavailability of flavan-3-ols and nutrigenomic response of apple polyphenols in minipigs challenged with a high fat meal. *Food and Function*, *6*(11), 5077–5090. https://doi.org/10.1039/d0fo00346h

Pérez, S., Mazeau, K., & Hervé du Penhoat, C. (2000). The three-dimensional structures of the pectic polysaccharides. *Plant Physiology and Biochemistry*,

38(1–2), 37–55. https://doi.org/10.1016/S0981-9428(00)00169-8

Pérez, S., Rodríguez-Carvajal, M. A., & Doco, T. (2003). A complex plant cell wall polysaccharide: Rhamnogalacturonan II. A structure in quest of a function. *Biochimie*, *85*(1–2), 109–121. https://doi.org/10.1016/S0300-9084(03)00053-1

Phan, A. D. T., Williams, B. A., Netzel, G., Mikkelsen, D., D'Arcy, B. R., & Gidley, M. J. (2020). Independent fermentation and metabolism of dietary polyphenols associated with a plant cell wall model. *Food and Function*, *11*(3), 2218–2230. https://doi.org/10.1039/c9fo02987g

Poncet-Legrand, C., Gautier, C., Cheynier, V., & Imberty, A. (2007). Interactions between flavan-3-ols and poly(L-proline) studied by isothermal titration calorimetry: Effect of the tannin structure. *Journal of Agricultural and Food Chemistry*, *55*(22), 9235–9240. https://doi.org/10.1021/jf071297o

R Core Team. (2014). A Language and Environment for Statistical Computing. *R Foundation for Statistical Computing*, *2*. Retrieved from http://www.r-project.org

Renard, C. M. G. C., Baron, A., Guyot, S., & Drilleau, J. F. (2001). Interactions between apple cell walls and native palle polyphenols/quantification and some consequences. *International Journal of Biology Macromolecules*, *29*, 115–125.

Renard, C. M. G. C., & Thibault, J. F. (1996). Pectins in mild alkaline conditions: β-elimination and kinetics of demethylation. *A.G.J. Voragen, J. Visser (Eds.), Progress in Biotechnology: 14 Pectins and Pectinases, Elsevier, Amsterdam*, *14*(C), 603–608. https://doi.org/10.1016/S0921-0423(96)80292-9

Ribas-Agustí, A., Martín-Belloso, O., Soliva-Fortuny, R., & Elez-Martínez, P. (2018). Food processing strategies to enhance phenolic compounds bioaccessibility and bioavailability in plant-based foods. *Critical Reviews in Food Science and Nutrition*, *58*(15), 2531–2548. https://doi.org/10.1080/10408398.2017.1331200

Ridley, B. L., O'Neill, M. A., & Mohnen, D. (2001). Pectins: Structure, biosynthesis, and oligogalacturonide-related signaling. *Phytochemistry*, *57*(6), 929–967. https://doi.org/10.1016/S0031-9422(01)00113-3

Rolland-Sabaté, A., Colonna, P., Potocki-Véronèse, G., Monsan, P., & Planchot, V. (2004). Elongation and insolubilisation of α-glucans by the action of Neisseria polysaccharea amylosucrase. *Journal of Cereal Science*, *40*(1), 17–30. https://doi.org/10.1016/j.jcs.2004.04.001

Rolland-Sabaté, A., Mendez-Montealvo, M. G., Colonna, P., & Planchot, V. (2008). Online determination of structural properties and observation of deviations from power law behavior. *Biomacromolecules*, *9*(7), 1719–1730. https://doi.org/10.1021/bm7013119

Saura-Calixto, F. (2011). Dietary fiber as a carrier of dietary antioxidants: An essential physiological function. *Journal of Agricultural and Food Chemistry*, *59*(1), 43–49. https://doi.org/10.1021/jf1036596

Schols, H. A., Bakx, E. J., Schipper, D., & Voragen, A. G. J. (1995). A xylogalacturonan subunit present in the modified hairy regions of apple pectin. *Carbohydrate Research*, *279*, 265–279. https://doi.org/10.1016/0008-6215(95)00287-1

Simha, R. (1940). The Influence of Brownian Movement on the Viscosity of Solutions. *The Journal of Physical Chemistry*, *44*(1), 25–34.

Stoddart, R. W., Spires, I. P., & Tipton, K. F. (1969). Solution properties of polygalacturonic acid. *The Biochemical Journal*, *114*(4), 863–870. https://doi.org/10.1042/bj1140863

Tang, H. R., Covington, A. D., & Hancock, R. A. (2003). Structure-Activity Relationships in the Hydrophobic Interactions of Polyphenols with Cellulose and Collagen. *Biopolymers*, *70*(3), 403–413. https://doi.org/10.1002/bip.10499

Tudorache, M., & Bordenave, N. (2019). Phenolic compounds mediate aggregation of water-soluble polysaccharides and change their rheological properties: Effect of different phenolic compounds. *Food Hydrocolloids*, *97*, 1–6. https://doi.org/10.1016/j.foodhyd.2019.105193

Tudorache, M., McDonald, J.-L., & Bordenave, N. (2020). Gallic acid reduces the viscosity and water binding capacity of soluble dietary fibers. *Food and Function*,

11, 5866–5874. https://doi.org/10.1039/d0fo01200a

Vernhet, A., Carrillo, S., & Poncet-Legrand, C. (2014). Condensed tannin changes induced by autoxidation: Effect of the initial degree of polymerization and concentration. *Journal of Agricultural and Food Chemistry*, *62*(31), 7833–7842. https://doi.org/10.1021/jf501441j

Voragen, A. G. J., Coenen, G. J., Verhoef, R. P., & Schols, H. A. (2009). Pectin, a versatile polysaccharide present in plant cell walls. *Structural Chemistry*, *20*(2), 263–275. https://doi.org/10.1007/s11224-009-9442-z

Waskom, M. (2014). Seaborn: Statistical Data Visualization. Retrieved from http://stanford.edu/~mwaskom/software/seaborn/

Watrelot, A. A., Le Bourvellec, C., Imberty, A., & Renard, C. M. G. C. (2013). Interactions between pectic compounds and procyanidins are influenced by methylation degree and chain length. *Biomacromolecules*, *14*(3), 709–718. https://doi.org/10.1021/bm301796y

Watrelot, A. A., Le Bourvellec, C., Imberty, A., & Renard, C. M. G. C. (2014). Neutral sugar side chains of pectins limit interactions with procyanidins. *Carbohydrate Polymers*, *99*, 527–536. https://doi.org/10.1016/j.carbpol.2013.08.094

Watrelot, A. A., Renard, C. M. G. C., & Le Bourvellec, C. (2015). Comparison of microcalorimetry and haze formation to quantify the association of B-type procyanidins to poly-l-proline and bovine serum albumin. *LWT - Food Science and Technology*, *63*(1), 376–382. https://doi.org/10.1016/j.lwt.2015.03.064

Zanchi, D., Konarev, P. V., Tribet, C., Baron, A., Svergun, D. I., & Guyot, S. (2009). Rigidity, conformation, and solvation of native and oxidized tannin macromolecules in water-ethanol solution. *Journal of Chemical Physics*, *130*(24). https://doi.org/10.1063/1.3156020

Table 1. Chemical characteristics of the procyanidins and pectins. A) Composition (mg/g dry matter) of purified acetonic fraction from 'Marie Ménard' and 'Avrolles' apple. B) Composition ratios and pectin region % based on the mol % quantifiable neutral sugars, galacturonic acid and pectin macromolecular characteristics.

A

	PCA	$\overline{DP}n$	Purified PCA constitutive units (%)			EC	DHC	CQA	PCQ	FLV	Total phenolics
			CAT_t	EC_t	EC_{ext}						
Marie Ménard	680	9	1.5	9.1	89.4	19.4	8.6	34.8	0.5	7.5	751
Avrolles	723	79	0.1	1.2	98.7	0	2.2	6.1	1.3	0	733
Pooled SD	*7.9*	*0.3*	*0.004*	*0.3*	*0.3*	*0.3*	*0.6*	*0.1*	*0.02*	*0.05*	*8.6*

B

	Gal A/Rha	(Ara+Gal) /Rha	Ara/Gal	Xyl* (mg/g)	FA* (mg/g)	DM* (%)	DAc* (%)	$\overline{M}_w$ * ($\times 10^3$ g/mol)	$\overline{[\eta]}_z$ (mL/g)	$\overline{R}_{Hz}$ (nm)	$\bar{d}_{Happ}$ (g/mol/nm^3)
AP2	28.8	11.2	2.0	19.3	-	86	17	431	1018	50.4	3.1
AP3	34.6	10.5	2.0	20.6	-	77	15	149	635	31.9	6.2
AP6	27.0	6.6	2.0	11.9	-	95	16	217	265	34.6	21.7
BP2	43.5	37.0	8.4	1.4	8.1	83	67	147	462	28.5	6.7
BP3	55.1	20.4	6.1	1.1	4.3	90	73	117	470	23.9	5.3
BP6	45.3	8.6	3.5	1.1	2.2	81	67	65	198	18.4	18.7
KPR2	56.5	11.6	0.2	7.8	-	73	5	287	426	37.4	9.1
KPR3	66.7	10.2	0.3	4.5	-	75	3	285	500	43.8	8.8
KPR6	35.4	8.1	0.3	4.3	-	79	6	161	195	27.6	23.1
KPO2	91.0	7.3	0.5	9.1	-	82	2	80	258	21.8	20.7
KPO3	68.8	5.8	0.5	8.8	-	82	7	137	378	37.2	22.4
KPO6	42.5	3.9	0.5	6.5	-	81	4	79	289	36.7	56.0
Pooled SD	*2.5*	*0.7*	*0.1*	*1.1*	*0.1*	*3.3*	*1.3*	*11.3*	*15*	*1.1*	*0.5*

PCA: procyanidins, $\overline{DP}n$: number-average degree of polymerization of procyanidins, CAT_t: terminal (+)-catechin units, EC_t: terminal (-)-epicatechin units, EC_{ext}: extension

(-)-epicatechin units, EC: (-)-epicatechin as flavan-3-ol monomer, DHC: dihydrochalcones, CQA: 5′-caffeoylquinic acid, PCQ, p-coumaroylquinic acid, FLV: flavonols. Ratios are calculated using the yields of neutral sugar expressed in mol%. The ratio between different sugars can contribute to understand information on polymer levels. The ratios of Gal A / Rha, (Ara+Gal) / Rha and Ara / Gal are characteristic for pectin backbone homogalacturonan / rhamnogalacturonan contribution, the branching of RG and the proportion of arabinans / galactans, respectively. Xyl and FA are indicators for the presence of xylogalacturonans and ferulic acids, respectively. DM and DAc are the degree of methylation and acetylation, respectively. $\bar{M}_w$, weight-average molar mass. $\overline{[\eta]}_z$, z-average intrinsic viscosity. $\bar{R}_{Hz}$, z-average hydrodynamic radius. $\bar{d}_{Happ}=\overline{M_w}/(4\pi/3) * \bar{R}^3_{Hw}$, average apparent molecular density. AP: pectins from apple cell wall, BP: pectins from beet cell wall, KP: pectins from kiwifruit cell wall, Gal A: galacturonic acid, Rha: rhamnose, Ara: arabinose, Gal: galactose, pH values-: 2: pH 2.0, 3: pH 3.5, 6: pH 6.0. Maturity-: R: –Ripe, O: –Overripe. * data adapted from (Liu et al., 2021). Pooled SD: pooled standard deviation.

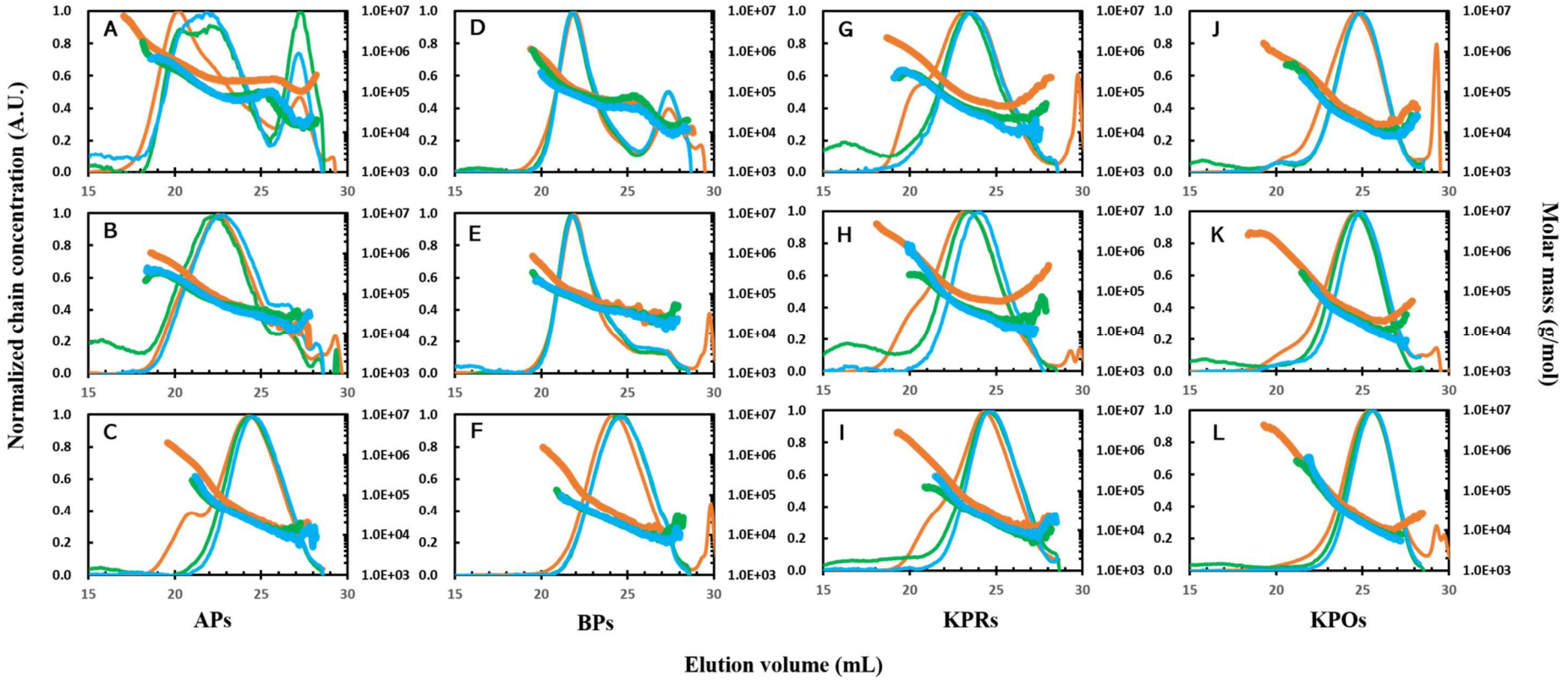

Fig. 1. HPSEC-MALLS chromatograms and molar mass *vs* elution volume of the pectin samples. A, B and C: AP2, AP3 and AP6, respectively; D, E and F: BP2, BP3 and BP6, respectively; G, H and I: KPR2, KPR3 and KPR6, respectively; J, K and L: KPO2, KPO3 and KPO6, respectively. Thin orange solid line ——: normalized chain concentration of pectins before interaction; Thin green solid line ——: normalized chain concentration of free pectins after interaction with DP9; Thin blue solid line ——: normalized chain concentration of free pectins after interaction with DP79. Orange thick solid line ——: molar mass of pectins before interaction; Green thick solid line ——: molar mass of free pectins after interaction with DP9; Blue thick solid line ——: molar mass of free pectins after interaction with DP79.

894 **Table 2** Relationships between molar masses and intrinsic viscosity.

Samples	Main peak		HMM region	
	M_i range (g/mol)	α	M_i range (g/mol)	α
AP2	2×10^5-2×10^6	0.55	NA	NA
AP3	2×10^4-2×10^5	1.17	2×10^5-2×10^6	0.34
AP6	2×10^4-2×10^5	1.07	5×10^5-5×10^6	0
BP2	5×10^4-2×10^5	1.04	2×10^5-2×10^6	0.12
BP3	5×10^4-2×10^5	1.16	10^5-10^6	0.41
BP6	10^4-10^5	0.96	10^5-10^6	0.17
KPR2	10^4-2×10^5	NA	2×10^5-2×10^6	0
KPR3	10^4-2×10^5	NA	2×10^5-2×10^6	0
KPR6	2×10^4-8×10^4	1.16	10^5-2×10^6	0
KPO2	10^4-7×10^4	1.02	10^5-10^6	0.41
KPO3	2×10^4-7×10^4	1.32	10^5-10^6	0.21
KPO6	10^4-6×10^4	0.94	6×10^4-10^6	0.17

895 HMM: high molar mass component. α: hydrodynamic coefficient for a given polymer calculated from
896 the Mark-Houwink -Sakurada equation $([\eta]_i = K_a M_i^{\alpha})$ for pectin samples in citrate/phosphate buffer
897 at pH 3.8, 0.1 M ionic strength. α = 0: Spheres, 0.5-0.8: Random coils, 1.0: Stiff coils, 2.0: Rods. NA:
898 Not applicable.

Table 3. Thermodynamic parameters of interactions between pectins (7.5 mM galacturonic acid equivalent) and procyanidins DP9 (A) and DP79 (60 mM (-)-epicatechin equivalent) (B) measured by Isothermal Titration Microcalorimetry (ITC).

A

DP9	n	Ka (M^{-1})	Δ H (kJ/mol)	Δ S (J/mol/K)	Δ G (kJ/mol)	-TΔS (kJ/mol)	Enthalpy (%)	Entropy (%)
AP2	0.081	4801	-5.18	53	-21	-16	25	75
AP3	0.108	2035	-1.32	59	-19	-18	7	93
AP6	-	-	-	-	-	-	-	-
BP2	0.088	2177	-1.88	58	-19	-17	10	90
BP3	-	-	-	-	-		-	-
BP6	-	-	-	-	-		-	-
KPR2	0.137	8160	-6.64	53	-22	-16	30	70
KPR3	0.071	4506	-3.34	59	-21	-18	16	84
KPR6	0.065	4554	-6.64	47	-21	-14	32	68
KPO2	0.111	12060	-6.20	57	-23	-17	27	73
KPO3	-	-	-	-	-	-	-	-
KPO6	-	-	-	-	-	-	-	-
Pooled SD	*0.02*	*242*	*0.55*	*4.5*	*0.7*	*0.6*	-	-

B

DP79	n	K_a (M^{-1})	Δ H (kJ/mol)	Δ S (J/mol/K)	Δ G (kJ/mol)	-TΔS (kJ/mol)	Enthalpy (%)	Entropy (%)
AP2	0.442	5588	-2.248	64	-21	-19	11	89
AP3	0.106	3582	-1.422	63	-20	-19	7	93
AP6	0.273	3183	-0.582	65	-20	-19	3	97
BP2	0.356	339	-1.861	42	-14	-13	13	87
BP3	0.614	351	-1.351	44	-15	-13	9	91
BP6	0.161	351	-2.278	39	-15	-12	15	85
KPR2	0.196	10649	-5.944	56	-23	-17	26	74
KPR3	0.100	2125	-2.187	56	-19	-18	12	88
KPR6	0.069	2715	-4.182	51	-19	-15	22	78
KPO2	0.210	12214	-8.019	51	-23	-15	35	65
KPO3	0.145	7090	-1.044	70	-22	-21	5	95
KPO6	0.093	7527	-3.893	61	-22	-18	18	82
Pooled SD	*0.04*	*443*	*0.35*	*6.3*	*0.5*	*0.4*	-	-

Average of duplicates for each. n: stoichiometry, K_a: affinity level, ΔH: enthalpy, ΔS: entropy, Δ G: free enthalpy, T: temperature. Enthalpy (%) = ΔH / (ΔH - TΔS) × 100%; Entropy (%) = - TΔS / (ΔH - TΔS) × 100%. Pooled SD: pooled standard deviation.

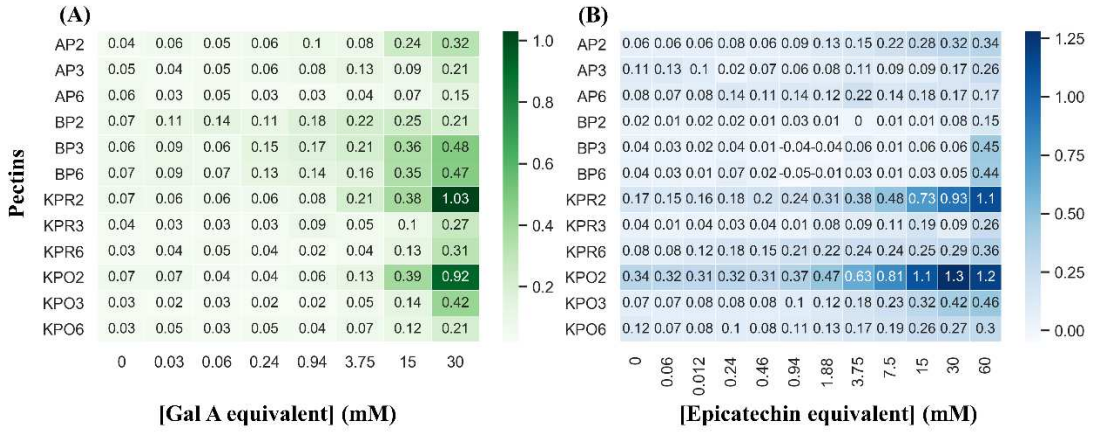

Fig. 2. Heat map of the turbidity characteristics of pectin-procyanidin DP9 interactions. Absorbance at 650 nm after interactions in 0.1 M citrate/phosphate buffer pH 3.8 (in triplicates). (A) Variation of absorbance of pectins at different concentrations (galacturonic acid equivalent) with procyanidins DP9 (60 mM (−)-epicatechin equivalent). (B) Variation of absorbance of procyanidins DP9 ((−)-epicatechin equivalent) at different concentrations with pectins (30 mM galacturonic acid).

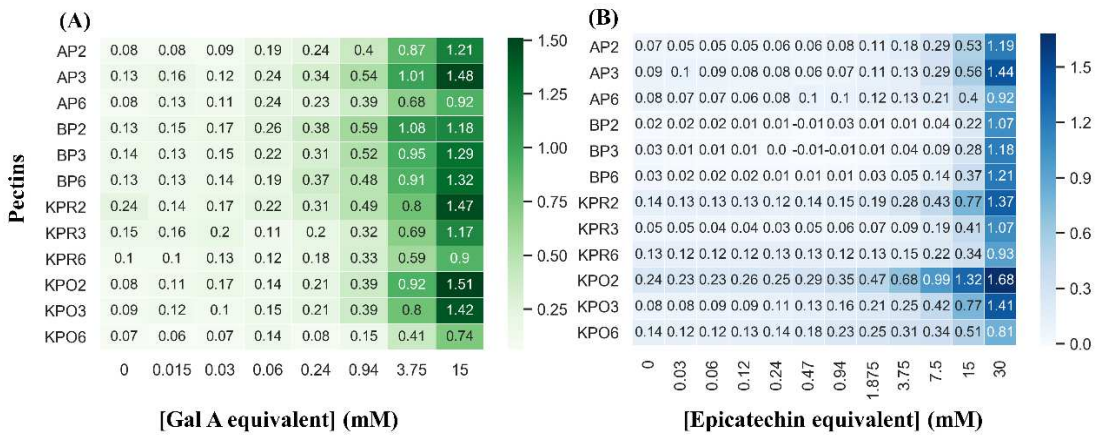

Fig. 3. Heat map of the turbidity characteristics of pectin-procyanidin DP79 interactions. Absorbance at 650 nm after interactions in 0.1 M citrate/phosphate buffer pH 3.8 (in triplicates). (A) Variation of absorbance of pectins at different concentrations (galacturonic acid equivalent) with procyanidins DP79 (30 mM (−)-epicatechin equivalent). (B) Variation of absorbance of procyanidins DP79 ((−)-epicatechin equivalent) at different concentrations with pectins (15 mM galacturonic acid).

Table 4. Changes in the molecular mass and concentrations of pectins and the degree of polymerization of procyanidins before and after interactions between pectic fractions and procyanidins DP9/79 (30/60 mM (-)-epicatechin equivalent).

Sample	Initial pectins $\overline{M}_w$ * ($\times 10^3$ g·mol^{-1})	Unbound pectins with PCA DP9		Unbound PCA DP9 with pectins	Unbound pectins with PCA DP79		Unbound PCA DP79 with pectins
		Concentration (g/l)	$\overline{M}_w$ ($\times 10^3$ g·mol^{-1})	$\overline{DP}n$ of free PCA	Concentration (g/l)	$\overline{M}_w$ ($\times 10^3$ g·mol^{-1})	$\overline{DP}n$ of free PCA
AP2	431	0.27 (2%[a])	165 (-266[b])	6 (-3[c])	0.44 (7%[a])	139 (-292[b])	39 (-40[c])
AP3	149	0.36 (3%)	104 (-45)	7 (-2)	0.39 (6%)	78 (-71)	39 (-40)
AP6	217	0.65 (5%)	37 (-180)	6 (-3)	0.60 (9%)	24 (-193)	41 (-38)
BP2	147	0.58 (3%)	99 (-48)	6 (-3)	0.58 (6%)	63 (-84)	33 (-46)
BP3	117	0.45 (3%)	75 (-42)	7 (-2)	0.52 (7%)	72 (-45)	39 (-40)
BP6	65	0.58 (5%)	22 (-43)	7 (-2)	0.50 (8%)	21 (-44)	27 (-52)
KPR2	287	0.51 (4%)	71 (-216)	7 (-2)	0.45 (7%)	49 (-238)	23 (-56)
KPR3	285	0.34 (4%)	62 (-223)	6 (-3)	0.20 (4%)	53 (-232)	26 (-53)
KPR6	161	0.62 (5%)	29 (-132)	7 (-2)	0.55 (9%)	29 (-132)	33 (-46)
KPO2	80	0.37 (3%)	32 (-48)	7 (-2)	0.51 (8%)	31 (-49)	31 (-48)
KPO3	137	0.57 (6%)	49 (-88)	5 (-4)	0.44 (9%)	36 (-101)	41 (-38)
KPO6	79	0.72 (6%)	35 (-44)	7 (-2)	0.69 (11%)	22 (-57)	40 (-39)
Pooled SD	*11.3*	*0.06*	*3.6*	*0.6*	*0.09*	*11.5*	*1.8*

*data adapted from Liu et al. (2020). Average of duplicates for each. $\overline{M}_w$: weight-average molar mass. $\overline{DP}n$: number-average degree of polymerization. [a] Pectin retention (%) = Unbound pectin concentration / Initial pectin concentration; [b] ΔM_w: difference of weight-average molar mass between pectic fractions unbound to procyanidin solutions after interaction with procyanidins and initial pectic fractions in buffer; [c] ΔDP_n: difference of degree of polymerization between procyanidins unbound to pectic fractions after interaction with pectins and initial procyanidins in buffer.

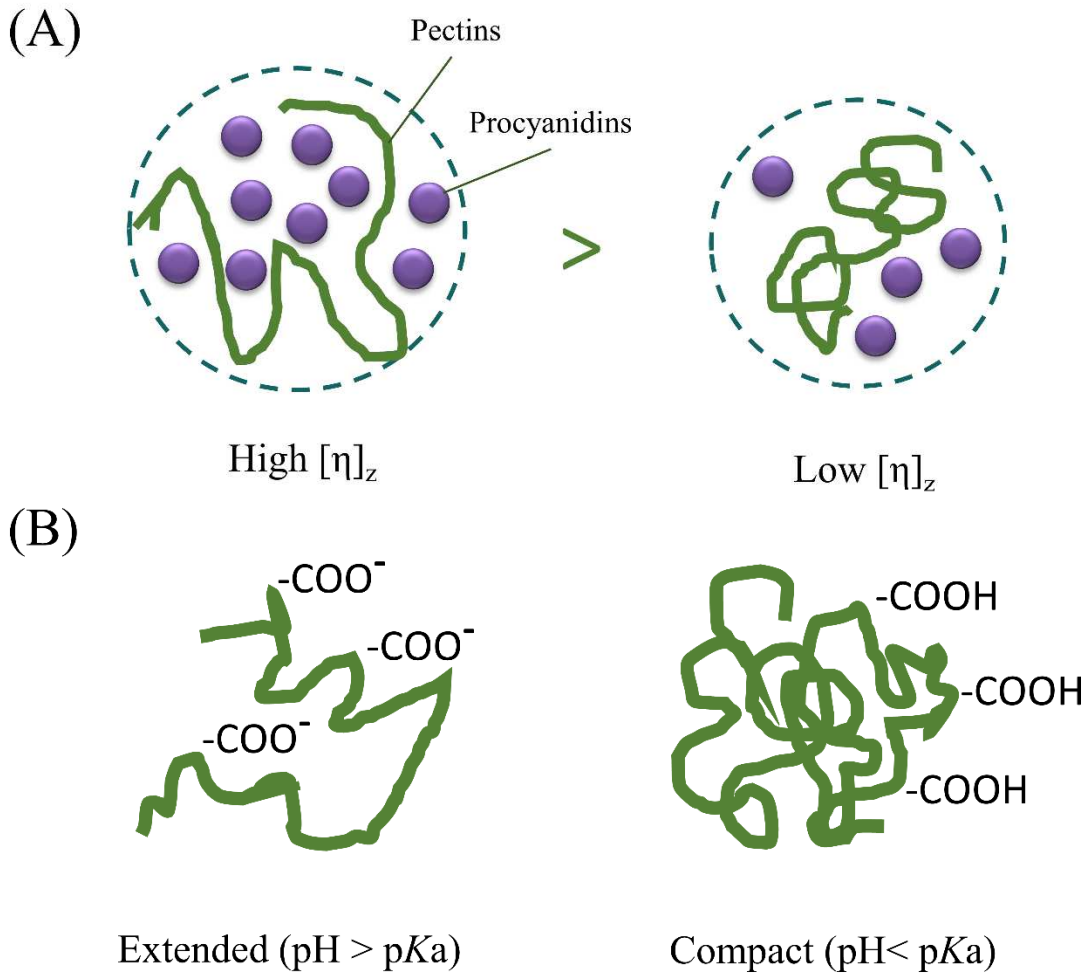

925
926 **Fig. 4.** (A) High and low intrinsic viscosity pectin chains, (B) Conformations of pectin chain extended
927 (pH > pKa) and compact (pH < pKa).

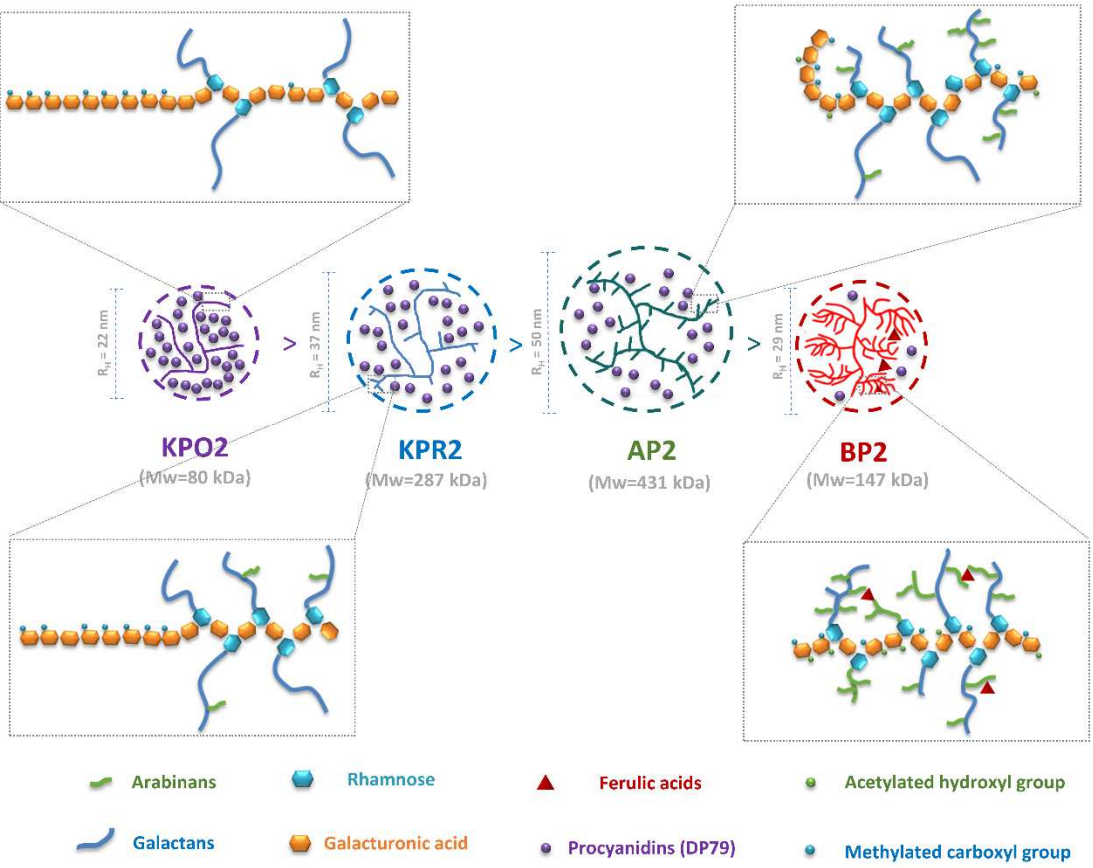

928

929 **Fig. 5.** Schematic representation of four populations of pectins adsorption of procyanidins DP79 and
930 the corresponding local details based on chemical composition and macromolecular characteristic data
931 (molar mass and hydrodynamic radius). Representation of KPO2 a linear polymer chain and less
932 branched polymer structures with KPR2 less long-chain branches, AP2 moderate RG content with
933 long/short-chain mixture branches, and BP2 both much RG region with short-chain and long-chain
934 branches, and some covalently bound ferulic acid.

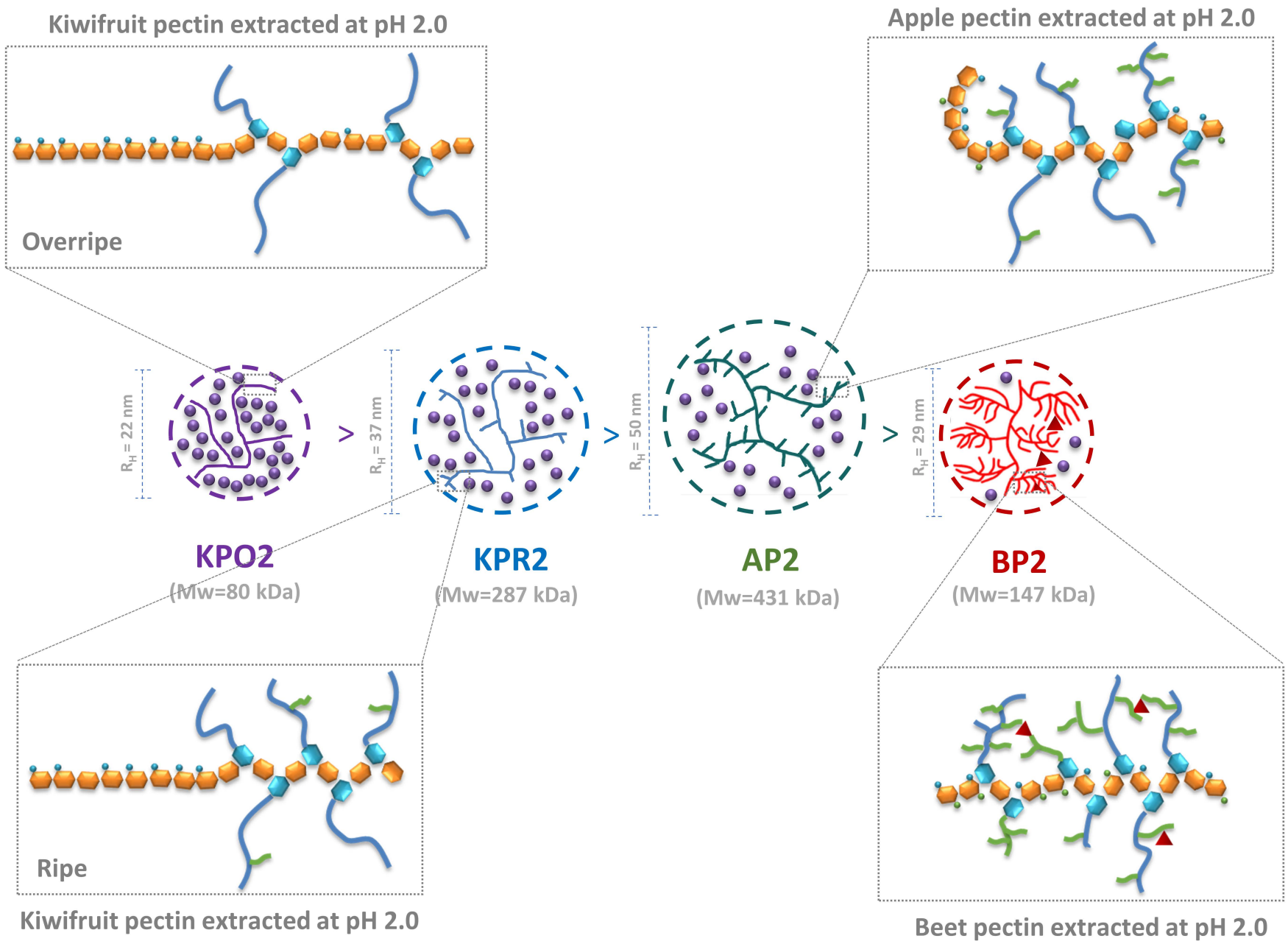
Kiwifruit pectin extracted at pH 2.0
Overripe
Apple pectin extracted at pH 2.0
R_H = 22 nm
>
R_H = 37 nm
>
R_H = 50 nm
>
R_H = 29 nm
KPO2
(Mw=80 kDa)
KPR2
(Mw=287 kDa)
AP2
(Mw=431 kDa)
BP2
(Mw=147 kDa)
Ripe
Kiwifruit pectin extracted at pH 2.0
Beet pectin extracted at pH 2.0
Arabinans
Galactans
Rhamnose
Galacturonic acid
Ferulic acids
Procyanidins (DP79)
Acetylated hydroxyl group
Methylated carboxyl group